CHAPTER 64

A NUMERICAL MODEL OF NEARSHORE CURRENTS BASED ON A FINITE AMPLITUDE WAVE THEORY

by

Masataka Yamaguchi*

ABSTRACT

A numerical model of wave-induced nearshore currents taking into account the finite amplitude effect is developed, with a cnoidal wave theory used for the estimation of wave characteristics. The model is applied to the computation of wave transformation and nearshore currents on uniformly sloping beaches and on two-dimensional model topographies. The comparison with the results obtained by a linear model shows that wave nonlinearity has a strong influence on wave transformation in shoaling water and in the surf zone and on the strength of nearshore circulation, but that it does not have much effect on the longshore current profile. Moreover, the validity of the present model is supported by the quantitative agreement with the experiment for wave height variations, and the qualitative correspondence with the experiment for mean water level variation and longshore currents and the observation for nearshore currents.

1. INTRODUCTION

In most nearshore current models, the small amplitude wave theory has been used for the calculation of wave transformation in shoaling water, the resulting radiation stress which is a driving force of nearshore currents, and the wave-induced bottom shear stress. Since the effect of wave nonlinearity becomes more and more predominant just outside and inside of the surf zone, a nearshore current model taking account of the finite amplitude effect is needed for the purpose of better understanding and description of the coastal phenomena. Nevertheless, there have not been any such numerical models of nearshore currents applicable to an arbitrary bottom topography, although a few analytical models by James(1974) and Tsuchiya et al.(1979) using a finite amplitude wave theory, are available.

Because of the above-mentioned situation, the aim of this study is to develop a numerical model of nearshore currents taking the effect of wave nonlinearity into account, in which cnoidal wave theories derived by both the Stokes first and second definitions for wave celerity are used for the estimation of wave characteristics and to clarify the model behaviour and its applicability by comparison with the results based on a linear numerical model, experiments of wave transformation and longshore currents and observations of nearshore currents.

* Prof., Dept. of Ocean Eng., Ehime Univ., Bunkyocho 3, Matsuyama 790, Ehime Pref., Japan

2. MODEL DESCRIPTION

(1) Wave transformation model

When the waves with wave number components (k_x, k_y) propagate on two-dimensional current (U,V), the governing equations of wave number components are derived from the irrotational condition of wave number components, the conservation equations of wave number components and the nonlinear dispersion relation of finite amplitude wave theory as

$$\begin{aligned}
&\frac{\partial k_x}{\partial t}+\frac{\partial}{\partial x}\left\{k_x\left(\frac{\partial \sigma_m}{\partial k}\cos\theta+U\right)\right\}+\frac{\partial}{\partial y}\left\{k_x\left(\frac{\partial \sigma_m}{\partial k}\sin\theta+V\right)\right\}\\
&=k_x\left[\frac{\partial\{(\partial\sigma_m/\partial k)\cos\theta\}}{\partial x}+\frac{\partial\{(\partial\sigma_m/\partial k)\sin\theta\}}{\partial y}\right]\\
&\quad+k_x\frac{\partial V}{\partial y}-k_y\frac{\partial V}{\partial x}-\frac{\partial\sigma_m}{\partial D}\frac{\partial D}{\partial x}-\frac{\partial\sigma_m}{\partial H}\frac{\partial H}{\partial x}\\
&\frac{\partial k_y}{\partial t}+\frac{\partial}{\partial x}\left\{k_y\left(\frac{\partial \sigma_m}{\partial k}\cos\theta+U\right)\right\}+\frac{\partial}{\partial y}\left\{k_y\left(\frac{\partial \sigma_m}{\partial k}\sin\theta+V\right)\right\}\\
&=k_y\left[\frac{\partial\{(\partial\sigma_m/\partial k)\cos\theta\}}{\partial x}+\frac{\partial\{(\partial\sigma_m/\partial k)\sin\theta\}}{\partial y}\right]\\
&\quad+k_y\frac{\partial U}{\partial x}-k_x\frac{\partial U}{\partial y}-\frac{\partial\sigma_m}{\partial D}\frac{\partial D}{\partial y}-\frac{\partial\sigma_m}{\partial H}\frac{\partial H}{\partial y}
\end{aligned}\tag{1}$$

in which k is the wave number, θ the wave direction, $\partial\sigma_m/\partial k$ the propagation velocity corresponding to the group velocity in the case of small amplitude wave theory, σ_m the relative angular frequency, $D(=h+\eta)$ the total water depth including the mean water level variation η, h the still water depth and H the wave height. It is seen that the effect of wave nonlinearity is introduced into eq. (1) explicitely through $(\partial\sigma_m/\partial H)\partial H/\partial x$ and $(\partial\sigma_m/\partial H)\partial H/\partial y$ and implicitely through $\partial\sigma_m/\partial k$ and $\partial\sigma_m/\partial D$. The equations are written in the conservative form for the convenience of their numerical integration using a finite difference method.

The energy balance equation with the energy dissipation term due to wave breaking is given by Phillips(1969) as

$$\begin{aligned}
&\frac{\partial}{\partial t}\left(E_n-\frac{M_x^2+M_y^2}{2\rho D}\right)+\frac{\partial}{\partial x}\left(UE_n+F_x-\frac{M_x^2+M_y^2}{2\rho D}\tilde{U}\right)\\
&+\frac{\partial}{\partial y}\left(VE_n+F_y-\frac{M_x^2+M_y^2}{2\rho D}\tilde{V}\right)+S_{xx}\frac{\partial U}{\partial x}+S_{xy}\frac{\partial V}{\partial x}\\
&+S_{yx}\frac{\partial U}{\partial y}+S_{yy}\frac{\partial V}{\partial y}-\frac{M_x}{\rho D}\frac{\partial S_{xx}}{\partial x}-\frac{M_y}{\rho D}\frac{\partial S_{xy}}{\partial x}\\
&-\frac{M_x}{\rho D}\frac{\partial S_{yx}}{\partial y}-\frac{M_y}{\rho D}\frac{\partial S_{yy}}{\partial y}=-E_{bw}
\end{aligned}\tag{2}$$

in which E_n is the wave energy, M_x and M_y the wave-induced mass flux components, $\tilde{U}$ and $\tilde{V}$ the nearshore current components including the effect of mass flux, F_x and F_y the energy flux components, S_{xx}, S_{xy} and S_{yy} the radiation stress tensor including the effect of mass flux and ρ the density of fluid. The nearshore current components and the integral properties are defined by the following expressions.

$$
\begin{aligned}
&\tilde{U}=U+M_x/\rho D,\ \tilde{V}=V+M_y/\rho D\\
&M_x=M\cos\theta,\ M_y=M\sin\theta,\ M=\overline{\int_{-D}^{\xi}\rho u dz}\\
&E_n=E_p+E_k,\ E_p=\rho g\overline{\xi^2}/2,\ E_k=\overline{\int_{-D}^{\xi}\rho(u^2+w^2)dz}/2\\
&F_x=F\cos\theta,\ F_y=F\sin\theta\\
&F=\overline{\int_{-D}^{\xi}\{\rho(u^2+w^2)/2+p+\rho gz\}udz}\\
&S_{xx}=S_{11}\cos^2\theta+S_{22}\sin^2\theta-M_x^2/\rho D\\
&S_{xy}=S_{yx}=(S_{11}-S_{22})\cos\theta\sin\theta-M_xM_y/\rho D\\
&S_{yy}=S_{11}\sin^2\theta+S_{22}\cos^2\theta-M_y^2/\rho D\\
&S_{11}=\overline{\int_{-D}^{\xi}(\rho u^2+p)dz}-\rho gD^2/2,\quad S_{22}=\overline{\int_{-D}^{\xi}pdz}-\rho gD^2/2
\end{aligned}
\tag{3}
$$

in which ξ is the surface displacement, u and w the wave-induced horizontal and vertical water particle velocity components, p the wave pressure, g the acceleration of gravity, E_p the potential energy, E_k the kinetic energy, and the overbar means time average over one wave period.

The estimation of energy dissipation due to wave breaking is done by either of two methods. The first one is to assume that the wave height exceeding the breaking wave height specified by the local characteristics of waves and water depth does not exist in the surf zone, and the breaker index used for the estimation of breaking wave height is

$$
\frac{H_{br}}{L_{br}}=a\tanh\frac{2\pi D_{br}}{L_{br}} \tag{4}
$$

in which L is the wave length and subscript 'br' means breaking waves. The coefficient in eq. (4) is the constant depending on the beach slope i, and a=0.131 for i=1/50 and a=0.142 for i=1/30 are chosen from the consideration of the Goda breaker index respectively.

The second method is to rely on the bore model proposed by Battjes (1978). The energy dissipation rate due to wave breaking is expressed as

$$
E_{bw}=\frac{B}{4\gamma^3}\frac{\rho gH^2\sqrt{gD}}{L}\left(\frac{H}{D}\right)^4,\ \gamma=0.7+5\,i \tag{5}
$$

The coefficient for i<1/20 is given by Iwagaki et al.(1981) as

$$
B=\begin{cases}11-10\,D/D_{br}\,; & 0.6\leq D/D_{br}\leq 1\\ 5 & ;\ D/D_{br}\leq 0.6\end{cases} \tag{6}
$$

In the numerical computation, the beach slope including the water surface slope $\partial D/\partial x$ is used rather than the beach slope itself.

(2) Nearshore current model

The equations used in the computation of nearshore currents are vertically-integrated continuity and momentum equations and they are written as

$$\frac{\partial \rho D}{\partial t}+\frac{\partial \tilde{M}_x}{\partial x}+\frac{\partial \tilde{M}_y}{\partial y}=0$$

$$\frac{\partial \tilde{M}_x}{\partial t}+\frac{\partial}{\partial x}(\tilde{U}\tilde{M}_x)+\frac{\partial}{\partial y}(\tilde{U}\tilde{M}_y)=-\rho g D\frac{\partial \eta}{\partial x}+\frac{\partial}{\partial x}\left(\bar{L}D\frac{\partial \tilde{U}}{\partial x}\right)$$

$$+\frac{\partial}{\partial y}\left(\bar{L}D\frac{\partial \tilde{U}}{\partial y}\right)-\left(\frac{\partial S_{xx}}{\partial x}+\frac{\partial S_{xy}}{\partial y}+\tau_{bx}\right) \quad (7)$$

$$\frac{\partial \tilde{M}_y}{\partial t}+\frac{\partial}{\partial x}(\tilde{V}\tilde{M}_x)+\frac{\partial}{\partial y}(\tilde{V}\tilde{M}_y)=-\rho g D\frac{\partial \eta}{\partial y}+\frac{\partial}{\partial x}\left(\bar{L}D\frac{\partial \tilde{V}}{\partial x}\right)$$

$$+\frac{\partial}{\partial y}\left(\bar{L}D\frac{\partial \tilde{V}}{\partial y}\right)-\left(\frac{\partial S_{yx}}{\partial x}+\frac{\partial S_{yy}}{\partial y}+\tau_{by}\right)$$

in which $\tilde{M}_x=\rho D\tilde{U}$, $\tilde{M}_y=\rho D\tilde{V}$.
The Longuet-Higgins expression(1970) is used as the lateral mixing term.

$$\bar{L}=N_c\rho l_x\sqrt{gD} \quad (8)$$

in which l_x is the distance measured from the shoreline and N_c the lateral mixing coefficient. The bottom shear stress is assumed to be proportional to the squared velocity, taking the wave orbital velocity into account. The definition of bottom shear stress components are given in

$$\tau_{bx}=\rho c_f(u_b\cos\theta+U)\sqrt{\overline{(u_b\cos\theta+U)^2+(u_b\sin\theta+V)^2}}$$
$$\tau_{by}=\rho c_f(u_b\sin\theta+V)\sqrt{\overline{(u_b\cos\theta+U)^2+(u_b\sin\theta+V)^2}} \quad (9)$$

in which C_f is the bottom friction coefficient in the wave-current system. Eq. (9) is numerically integrated by the Causs-Legendre formula in each iterative computation. In the actual simulation, the values of N_c and C_f are fixed to be 0.01 and 0.01 respectively.

3. WAVE CHARACTERISTICS AND INTECRAL PROPERTIES OF CNOIDAL WAVES

In the model, the wave characteristics and integral properties of waves are estimated from the second order solutions of the cnoidal wave theories derived using both the Stokes first and second definitions for wave celerity by Chappelear(1962) and by Tsuchiya & Yamaguchi(1972).

The wave characteristics based on the Chappelear theory using the first definition for wave celerity are given for wave celerity c, wave length L and horizontal water particle velocity at the bottom u_b as

$$c/\sqrt{gD}=1+L_3+L_0(1-e)+5L_0L_3(1-e)+L_0^2\{5+4\kappa^2-5(1+\kappa^2)e\}/3$$

$$L/D=4K/\sqrt{3L_0} \quad (10)$$

$$u_b/\sqrt{gD}=L_0(1-e)+L_0^2(5+4\kappa^2)/3-5L_0^2(1+\kappa^2)e/3+5L_0L_3(1-e)$$
$$-\{L_0\kappa^2+L_0^2\kappa^2(1+\kappa^2)+5L_0L_3\kappa^2\}\mathrm{sn}^2\beta x-L_0^2\kappa^4\mathrm{sn}^4\beta x$$

in which κ the modulus of the Jacobian elliptic function, e=E/K, K and E the complete elliptic integrals of the first and second kinds, sn the Jacobian elliptic function and $\beta x=2K(x-ct)/L$. The expansion parameters L_0 and L_3 in the above expressions can be obtained from the following equations as a function of κ and H/D.

$$L_0\kappa^2\{1+L_0(10+7\kappa^2)/4+6L_2\}=H/D$$
$$2L_2+L_0(\kappa^2+e)+L_0^2\{-(1-6\kappa^2-9\kappa^4)/5+2(1+\kappa^2)e\}+6L_0L_2(\kappa^2+e)+L_2^2=0 \tag{11}$$

Considering the relation that $\sigma_m\sqrt{D/g}=(c/\sqrt{gD})kD$, the partial derivatives in eq. (1) can be computed from

$$\frac{1}{\sqrt{gD}}\frac{\partial\sigma_m}{\partial k}=\frac{-2\pi}{k^2D^2}\frac{\partial\{(c/\sqrt{gD})kD\}}{\partial(L/D)}$$
$$\sqrt{\frac{D^3}{g}}\frac{\partial\sigma_m}{\partial D}=-\frac{1}{2}\frac{c}{\sqrt{gD}}kD-\frac{H}{D}\frac{\partial\{(c/\sqrt{gD})kD\}}{\partial(H/D)}-\frac{L}{D}\frac{\partial\{(c/\sqrt{gD})kD\}}{\partial(L/D)} \tag{12}$$
$$\sqrt{\frac{D^3}{g}}\frac{\partial\sigma_m}{\partial H}=\frac{\partial\{(c/\sqrt{gD})kD\}}{\partial(H/D)}$$

These expressions are estimated by the numerical differentiation of $\sigma_m\sqrt{D/g}$ computed as a function of L/D and H/D.

The integral properties of the cnoidal waves were calculated by Yamaguchi(1977). However, it was found that the results for mass flux and radiation stress are not sufficient in order estimation. Recalculation of these properties was attempted by using the exact relations between the integral properties of finite amplitude waves. For example, the exact relation derived by Crapper(1979) was used in the calculation of radiation stress.

$$S_{11}=4E_k-3E_p+\rho D\overline{u_b^2},\quad S_{22}=E_k-E_p+\rho D\overline{u_b^2}/2 \tag{13}$$

Fig. 1 shows two examples of the wave characteristics and integral properties non-dimensionalized by the results based on the small amplitude wave theory. The dimensionless propagation velocity $\widehat{\partial\sigma_m/\partial k}$ in-

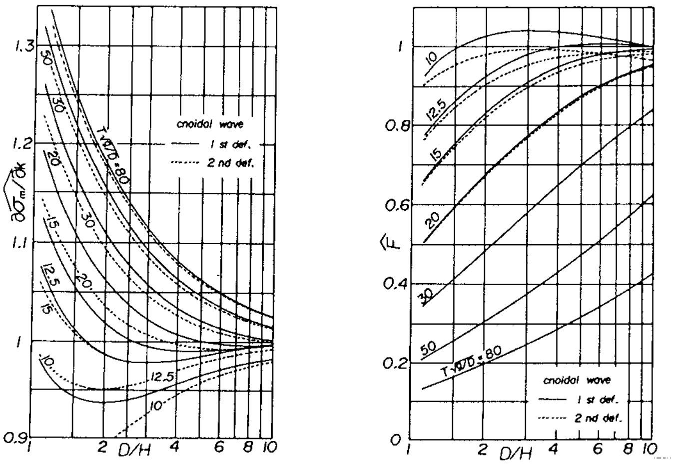

Fig. 1 Examples of wave characteristics and integral properties of cnoidal waves.

creases and the dimensionless energy flux $\hat{F}$ decreases with increasing values of $T\sqrt{g/D}$ and H/D in the case of larger values of $T\sqrt{g/D}$. The effect of the definitions for wave celerity on the wave characteristics and integral properties becomes more significant in the case of smaller values of $T\sqrt{g/D}$ and D/H, and the difference becomes negligible with the increase of these parameters. It is noted that the small amplitude wave theory overestimates or underestimates the wave characteristics including the integral properties of waves and that because of the limitation to practical applicability, the cnoidal wave theory should be used in the range of $T\sqrt{g/D}>12$.

4. NUMERICAL MODEL OF NEARSHORE CURRENTS

(1) Finite difference formulation

A finite difference method is used to solve the governing equations. Fig. 2 is the coordinate system used, in which x axis and y axis are taken in the offshore direction and in the longshore direction respectively. Finite difference approximation for the equations of wave number components and the energy balance equation which constitute the wave transformation model is made by forward difference in time and x direction and by central difference in y direction. The continuity and momentum equations which make up the nearshore current model are discretized by the forward difference with respect to the time variable and by the central difference with respect to the space variables, and finite differencing of these equations is lagged a half step in time. Fig. 3 shows the configuration of variables in the finite difference model. Current components and bottom shear stresses are defined on the grid sides and all other variables are estimated at the grid center.

The initial condition and the conditions for the offshore fixed boundary used in the nearshore current model are the usual ones. In the longshore direction, the periodic boudary condition proposed by E. Noda (1974) is imposed on all the variables relevant to the computation. In

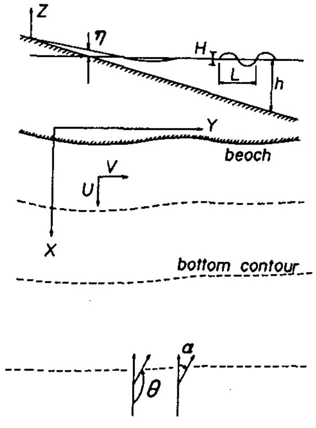

Fig. 2 Coordinate system used in nearshore current model.

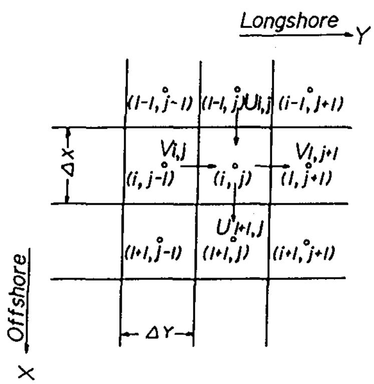

Fig. 3 Configurations of variables in finite difference model.

the wave transformation model, the specified values of wave characteristics are given at the offshore boundary, but any conditions of wave characteristics at an onshore boundary are not required in the case of a straight shoreline because of the property of the finite difference method used.

The computer program starts with determining the spatial distribution of wave characteristics according to the analytical solution of wave transformation on the parallel bottom contour based on the small amplitude wave theory, and the wave characteristics at the first step are computed from the nonlinear wave transformation model. Then, the nearshore current computation is carried out using the radiation stress estimated from the wave transformation model. Thus, one iteration is completed by these computations.

A steady state solution is obtained by 1400 to 2000 iterations of alternating computations between wave transformation and nearshore currents. At an early stage of iterative computation, the input wave height is increased gradually in order to avoid the appearance of numerical instability and to accelerate the convergence to a steady state solution. In the computation of wave transformation, the energy dissipation due to wave breaking is estimated by either the bore model or the breaker index model, when the wave height exceeds the breaking wave height given by eq. (4).

(2) Interpolation of wave characteristics

The wave information obtained directly from each computation of wave transformation is k_x, k_y (L and θ) and E_s ($=E_n - M^2/2\rho D$). When the small amplitude wave theory is used, the effect of mass flux is usually neglected and then the wave height is easily computed from the relation that $E_n=(1/8)\rho g H^2$. On the contrary, when a cnoidal wave theory is used, it is not easy to transform from E_s to H and the numerical computation of the other wave characteristics is also time-consuming, because their expressions are lengthy and contain the elliptic integrals.

In this study, the following method is adopted to save computer processing time. First, the numeric tables of the wave characteristics including the integral properties of waves computed in the range of $L/D=5-150$ every 1 increment and of $H/D=0.01-1.30$ every 0.01 increment are prepared in advance. The wave characteristics tabulated are $c/\sqrt{gD}$, $(\partial\sigma_m/\partial k)/\sqrt{gD}$, $\sqrt{D^3/g}\,\partial\sigma_m/\partial D$, $\sqrt{D^3/g}\,\partial\sigma_m/\partial H$, $E_n/(\rho g D^2/8)$, $E_s/(\rho g D^2/8)$, $M/\rho D\sqrt{gD}$, $S_{11}/\rho g D^2$, $S_{22}/\rho g D^2$, $F/(\rho g D^2\sqrt{gD})$, and κ, L_0, L_3, K and E required in the computation of u_b. Next, a two-dimensional linear interpolation formula is applied to estimate the wave characteristics corresponding to the values of L/D and H/D obtained in each iteration.

$$
\begin{aligned}
&f=a'f_{i,j}+b'f_{i,j+1}+c'f_{i+1,j}+d'f_{i+1,j+1}\\
&a'=(1-r)(1-s),\ b'=r(1-s),\ c'=(1-r)s,\ d'=rs\\
&i=[L/D],\ \ j=[100(H/D)]\\
&r=L/D-[L/D],\ \ s=100(H/D)-[100(H/D)]
\end{aligned}
\tag{14}
$$

in which f is the interpolated value, $f_{i,j}$ the value of f on the numeric table for the i-th L/D and the j-th H/D and [ ] the Gauss's symbol. The computation of sn function in the expression of u_b is obtained through the theta function in the usual manner, although an approximation such as $\mathrm{sn}\,\beta x \approx \tanh \beta x$ is used in the case of $\kappa>1-10^{-6}$

A similar method can be used in the conversion of E_s to H. As $E_s/(\rho g D^2/8)$ is a function of H/D for a fixed L/D, the numeric table of H/D inverted as a function of $E_s/(\rho g D^2/8)$ can be made by applying the linear interpolation formula to the numeric table of $E_s/(\rho g D^2/8)$. Two kinds of tables of H/D given as a function of L/D and $E_s/(\rho g D^2/8)$ are produced to keep the accuracy of interpolated results and to save computer storage memory, in which the range of $E_s/(\rho g D^2/8)$ are 0.001 - 0.15(0.001 increment) and 0.15 - 1.50(0.01 increment) respectively.

After all, the value of H/D corresponding to L/D and $E_s/(\rho g D^2/8)$ computed in each iteration can be interpolated from the H/D-tables, and then the wave characteristics for L/D and H/D can be evaluated by the application of the linear interpolation formula, eq.(14). It is emphasized that since this method is applicable for not only a cnoidal wave theory but also another higher order finite amplitude wave theory, the incorporation of the theory into a nearshore current model is easily possible for its improvement.

5. COMPUTATIONAL RESULTS AND CONSIDERATION

(1) Uniformly sloping beach

The computation is carried out on a plane beach with the slope of 1/30 and constant water depth of h=8 m in the offshore region. The following input conditions are used; the incident wave height H_M=2 m, the wave period T_M=12.5 s and the incident angle of waves $\alpha_M(=\pi-\theta_M)=30°$. Suffix 'M' means the value at the offshore boundary.

In Fig. 4, the results in the nonlinear model are depicted with those in the linear model developed by the authors(1983). Rapid increase of the wave height before wave breaking due to nonlinear shoaling and rapid decay of the wave height due to wave breaking are observed in the nonlinear model using the bore model, and the wave height after wave

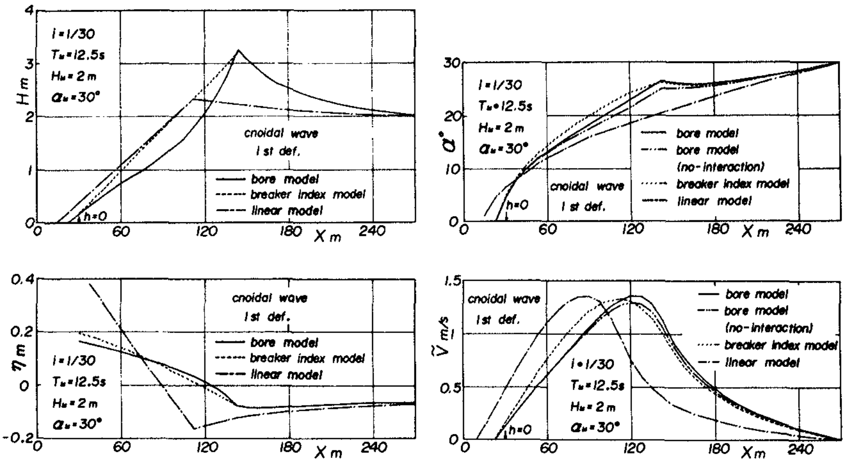

Fig. 4 Change of wave height, wave direction and mean water level variation and longshore current profile on a uniformly sloping beach.

breaking based on the bore model diminishes more rapidly than that based on the breaker index model. While the wave direction in the linear model decreases steadily toward the shore, the wave direction in the nonlinear model slightly increases just before wave breaking and it decreases steadily as well after wave breaking. This is mainly due to the wave-current interaction, because the tendency almost disappears when the effect of the interaction is omitted in the computation.

The wave setup and setdown in the vicinity of the breaking point in the linear model is much greater than those in the nonlinear model, because the small amplitude wave theory overestimates the radiation stress in comparison with a finite amplitude wave theory, as is well known. It is also interesting to note that the current profile and the magnitude in the nonlinear model are similar to those in the linear model, although the peak position of the current profile in the nonlinear model is at a greater water depth.

From the above argument, it is summarized that the wave nonlinearity has a strong influence on the offshore distribution of wave height, wave direction and mean water level variation, and the peak position of longshore currents, but that it does not have much effect on the longshore current profile itself.

Fig. 5 shows the results of wave height variation and the longshore current profile computed on a uniformly sloping beach with a longshore bar. The input conditions are the same as those for a uniformly sloping beach. It is assumed in the computation that the energy dissipation due to wave breaking does not occur on the inversely sloping beach. In the nonlinear model, the waves break after rapid increase of the wave height due to nonlinear shoaling on the offshore regularly sloping beach and propagate with loss of their heights on the inversely sloping beach. Then, the waves again increase their heights due to nonlinear shoaling on the onshore regularly sloping beach and finally dissipate their energy after the second wave breaking. On the other hand, in the linear model, the waves break on the onshore regularly sloping beach after gradual change of the wave height with water depth variation. As a result, the longshore current profile in the nonlinear model has a two peak structure, while the one in the linear model has a single peak structure as well as the result on a uniformly sloping beach.

Thus, it can be said that the correct estimation of the breaking point is of great importance in the longshore current prediction on a bar-trough beach profile.

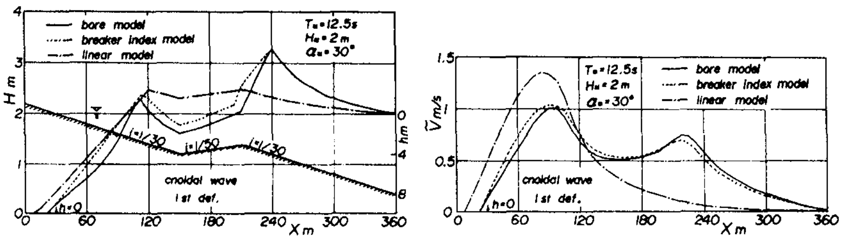

Fig. 5 Change of wave height and longshore current profile on a uniformly sloping beach with a longshore bar.

(2) Two-dimensional bottom topography

The bottom topography model developed by E. Noda(1974) is chosen to the computation of nearshore currents on a two-dimensional topography and it is expressed as

$$h(x,\ y)= ix\left[1+A_0\exp\left\{-3\left(\frac{x}{45}\right)^{1/2}\right\}\sin^2\left\{\frac{\pi}{\lambda}(y-x\tan\varepsilon)\right\}\right] \tag{15}$$

in which i is the mean beach slope of 0.015, λ the longshore beach length of 400 m, A_0 the maximum amplitude of the bottom undulation of 20 m and ε the skewness of the bottom undulation of 0° or 30°. It should be noted that the above expression has different constants from the original one by E. Noda(1974). The model topography with ε=0° and the one with ε=30° are referred to as symmetrical concave topography and asymmetrical concave topography respectively.

Fig. 6 describes the nearshore current pattern on a symmetrical concave topography with normal incidence of waves computed by both the linear and nonlinear models, in which the solid line is the contourline of water depth, and the dotted line indicates an approximate breaker line evaluated from eq. (4). Incident wave height H_M is 1 m and the other conditions are the same as in the case for a uniformly sloping beach. In both the figures, we can see the formation of a pair of dominant nearshore circulation cells centered on a breaking point and a pair of very weak and flat cells near the shoreline. But, the strength of current velocity in the nonlinear model is relatively weaker than that in the linear model and the center of the dominant circulation cell in the nonlinear model also locates in farther offshore region with the movement of the breaking point.

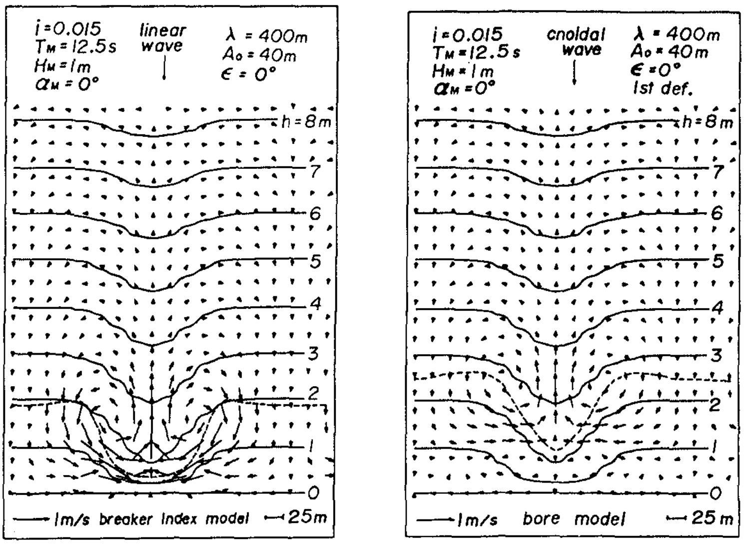

Fig. 6 Nearshore current pattern on symmetrical concave topography.

Fig. 7 is the nearshore current pattern on an asymmetrical concave topography with oblique incidence of waves, in the case where the input wave height H_M is 2 m. It is found in both the figures that the meandering longshore current is predominant and that a counterclockwise circulation cell is formed in the trough region near the shoreline by the effect of concave bottom topography. The scale and strength of a circulation cell in the linear model are greater than those in the nonlinear model.

It can be said from the two examples mentioned above that the wave nonlinearity acts so as to suppress the formation and growth of the nearshore circulation cell.

When a method combining a wave ray technique with a linear interpolation formula is used for the numerical integration of the equations of

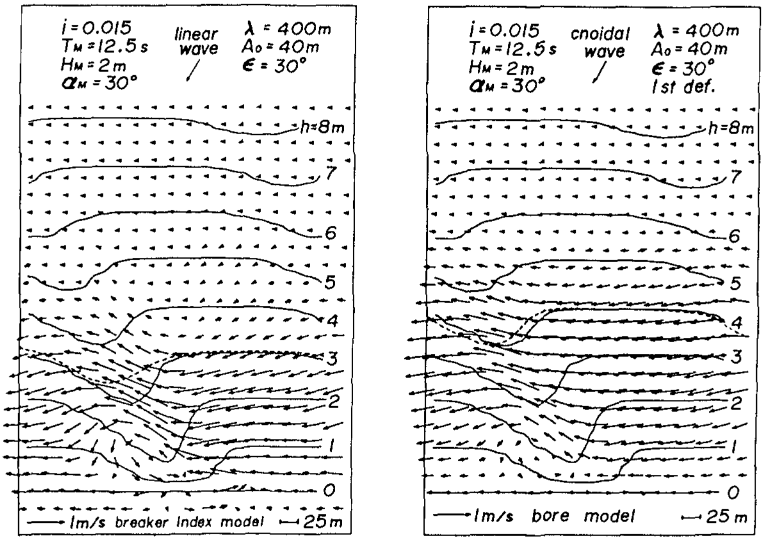

Fig. 7 Nearshore current pattern on asymmetrical concave topography.

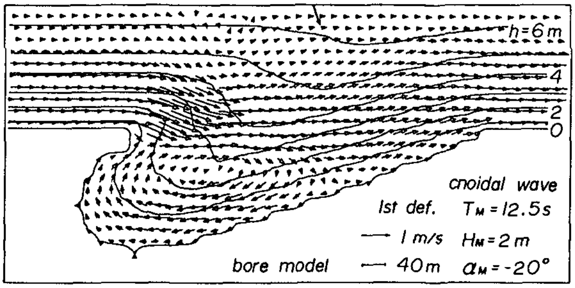

Fig. 8 Nearshore current pattern on curved bay.

wave number components and the energy balance equation, nearshore current pattern on a two-dimensional bottom topography with an arbitrary shoreline can be obtained as shown in Fig. 8, which demonstrates the predominant longshore currents in the outer region and a clockwise nearshore circulation in the inner region.

6. VERIFICATION OF NEARSHORE CURRENT MODEL

(1) Comparison with experiment

Fig. 9 is the comparison of the computed results with the experimental ones for the change of wave height and mean water level variation on a uniformly sloping beach of 1/34.26 conducted by Hansen & Svendsen(1979). As for the wave height variation, the result in the nonlinear model using a cnoidal wave theory of the second definition for wave celerity rather than the first definition for wave celerity gives slightly better agreement with the experiment, and the linear model can not explain rapid increase of wave height before wave breaking.

On the contrary, the nonlinear model underestimates the wave setdown and setup, although it can reproduce the qualitative trend in the experiment. In general, it has been known from experiments that the transition of wave setdown to setup does start from the plunge point rather than the breaking point. However, the present model, as well as the previous models, does not formulate this phenomena. The linear model overestimates the wave setdown in the vicinity of the breaking point and wave setup near the shoreline, although some fraction of the wave setup seems to agree well with the experimental results in appearance.

Fig. 10 indicates the comparison of the computed result with the experimental one for longshore currents on a uniformly sloping beach

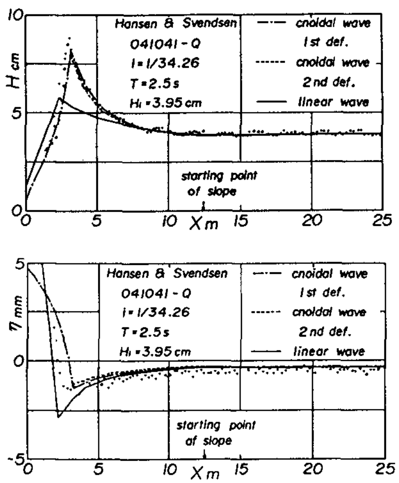

Fig. 9 Comparison between computation and experiment for wave height and mean water level variation.

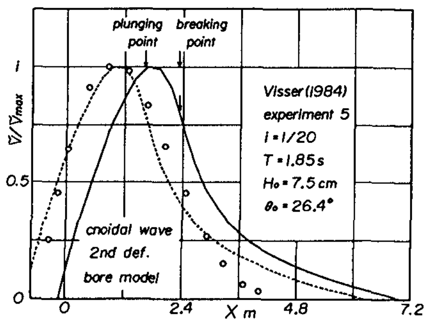

Fig. 10 Comparison between computation and experiment for longshore currents.

with the slope of 0.05 measured by Visser(1984). The current profile itself in the nonlinear model is similar to the experimental profile and the location of the breaking point in the model is in good agreement with that in the experiment. However, in order to get a close agreement with the experiment, the computed result has to be shifted toward the shoreward by approximately the amount of the plunge point distance.

(2) Comparison with observation

Fig. 11 shows the nearshore current pattern re-evaluated from the observation of transport velocity by Sonu(1972) and the corresponding nearshore current pattern computed by the nonlinear model. In the model, the energy dissipation due to wave breaking is estimated by the bore model, and a cnoidal wave theory based on the first definition is used. The input wave conditions given at the offshore boundary are that T_M=5 s, H_M =0.2 m and α_M=0°. The bottom topography used in the computation is slightly modified to be periodic in the longshore direction and to have a straight shoreline. The model reproduces well the qualitative features of the complicated nearshore current pattern found in the observation, such as the onshore currents in both sides of the region and the rip currents in the central part of the region. But, in a quantitative sense, the model appears to give less velocity than the observation.

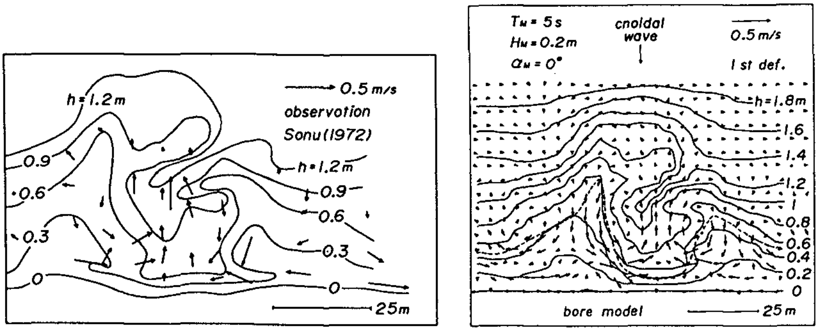

Fig. 11 Nearshore current pattern observed by Sonu(1972) and the corresponding result computed by the nonlinear model.

7. CONCLUSIONS

The main conclusions of this study are summarized as follows.

i) A nonlinear model of nearshore currents was developed, in which the estimation of wave characteristics is based on a cnoidal wave theory.

ii) The wave nonlinearity has a strong influence on the offshore distribution of wave height, wave direction and mean water level variation and the peak position of longshore currents, but it does not have much effect on the longshore current profile itself.

iii) The wave nonlinearity acts so as to suppress the formation and growth of nearshore circulation currents.

iv) The nonlinear model quantitatively predicts the change of wave height in shoaling zone and in the surf zone. It also qualitatively produces the mean water level variation, longshore current profile and nearshore circulation pattern.

v) It is necessary to make allowance for the effect of plunge point distance in the model formulation in order to obtain better agreement with the experimental data on wave setup and longshore currents.

8. ACNOWLEDGEMENT

Thanks are due to Mr. H. Kawahara, Graduate Course student of Ocean Engineering, Ehime University for his valuable help during the study. A part of this study was accomplished with the support of the Science Research Fund of the Ministry of Education, for which the authors express their appreciation.

9. REFERENCES

Battjes, J. A.: Energy dissipation in breaking solitary and periodic waves, Manus., Delft Univ. of Tech., 1978.

Chappelear, J. E.: Shallow-water waves, Jour. Geophys. Res., Vol. 67, No. 12, pp. 4693 - 4704, 1962.

Crapper, G. D.: Energy and momentum integrals for progressive capillary-gravity waves, Jour. Fluid Mech., Vol. 94, pp. 13 - 24, 1979.

Hansen, J. B. and I. A. Svendsen: Regular waves in shoaling water, experimental data, Inst. Hydrodyn. and Hydr. Eng, Series Paper 21, 1979.

Iwagaki, Y., Mase, H. and T. Tanaka: Modeling of irregular wave transformation in shoaling water, Proc. 28th Conf. on Coastal Eng. in Japan, pp. 104 - 108, 1981(in Japanese).

James, I. D.: A non-linear theory of longshore currents, Estuarine and Coastal Marine Sci., Vol. 2, pp. 235 - 249, 1974.

Longuet-Higgins, M. S.: Longshore currents generated by obliquely incident sea waves, 2, Jour. Geophys. Res., No. 33, pp. 6790 - 6801, 1970.

Noda, E. H.: Wave-induced nearshore circulation, Jour. Geophys. Res., Vol. 79, No. 27, pp. 4097 - 4106, 1974.

Phillips, O. M.: The Dynamics of the Upper Ocean, Camb. Univ. Press, p. 261, 1969.

Sonu, C. J.: Field observation of nearshore circulation and meandering currents, Jour. Geophys. Res., Vol. 77, No.18, pp. 3232 - 3246, 1972.

Tsuchiya, Y. and M. Yamaguchi: Some considerations on water particle velocity of finite amplitude wave theory, Coastal Eng. in Japan, Vol. 15, pp. 43 - 57, 1972.

Tsuchiya, Y., Yasuda,T. and K. Tokuda: Theory of rip currents (1) - case of normally incident waves -, Proc. 26th Conf. on Coastal Eng. in Japan, pp. 495 - 499, 1979(in Japanese).

Visser, P. J.: Uniform longshore current measurements and calculations, Proc. 19th International Conf. on Coastal Eng., Vol. III, pp. 2192- 2207, 1984.

Yamaguchi, M.: Some characteristics of finite amplitude waves, Memoirs of the Ehime Univ., Sect III(Eng), Vol.VIII, No. 4, pp. 191 - 202, 1977(in Japanese).

Yamaguchi, M., Tanabe, H. and Y. Nishioka: A numerical solution of near-shore currents taking account of wave-induced mass flux, Proc. 30th Conf. on Coastal Eng. in Japan, pp. 480 - 484, 1983(in Japanese).